

Nigerian Journal of Physics (NJP)

ISSN online: 3027-0936 ISSN print: 1595-0611

DOI: https://doi.org/10.62292/njp.v34i4.2025.431

Volume 34(4), December 2025



Application of Electrical Resistivity Tomography in Mapping the Lateral Extent of Ohia Kaolin Deposit in Umuahia Southeastern Nigeria

*¹Aigba Paul Igienekpeme, ²Amos-Uhegbu Chukwunenyoke, ¹Ugwu Joshua Udoka, ²Eze Martina Onyinye and ¹Chukwu Darlington Chinedu

¹Department of Physics, Michael Okpara University of Agriculture, Umudike. ²Department of Geology, Michael Okpara University of Agriculture, Umudike.

*Corresponding Author's Email: paul aigba@yahoo.co.uk

ABSTRACT

The Electrical Resistivity Tomography of Ohia community in Umuahia for eight (8) profiles located within the coordinates N5⁰31'49.8" E7⁰26'53.4" and N5⁰36'47.8" E7⁰26'50.9" using Integrated Geophysical Instrument (IGI) for kaolin mapping was carried out. The resistivities obtained from the readings were converted to apparent resistivities and plotted using the RESINVx64 software to infer the electrical responses of the subsurface at the injection of Direct Current (D.C.) through the current electrode of a higher potential. Wenner configuration that is characterized by equidistance between the potential-potential electrodes and the potential-current electrodes was deployed in view of the expected outcome which is the lateral extent of Kaolin deposit. Resistivity inversion of three iterations mapped the subsurface for its electrical responses. Different profiles have different kaolin signatures though with some similarities in some cases. ERT 1 and ERT 3 being deeply buried are close in terms of prospect similarities while ERT 3, ERT 4 and ERT 5 have some similarities in their prospect distributions as deposits become dense southwest ward though discontinuous. ERT 6 and ERT 7 follow similar depositional trend with massive overburden being deeply buried except that the latter has kaolin blended with other rocks. Accessibility to the prospect in ERT 8 would attract less investment because of its closeness to the surface. The lateral spread of kaolin is between 7.5 and 97.5 m with a depth of burial ranging from 1.25 to 9.26m.

Keywords:

Kaolin, Lateral extent, Permeability, Electric current density, Equipotential lines.

INTRODUCTION

Electrical Resistivity Tomography (ERT) also known as Electrical Resistivity Imaging (ERI) is a subsurface profilling technique that showcases the electrical responses of various rock layers when a direct current or low frequency alternating currents is passed into the subsurface through current electrodes. Naturally occurring elements in uncombined form having distinct minerals structure and graphite allow the drift of electrons for electricity conduction. Majority of minerals that make up rocks are insulators with poor conduction. In view of this, conduction is carried out electrolytically rather than electronically because pore water ions carry out the conduction. In rocks, porosity is the main control of rock resistivity, with both not having direct relationship. Intergrannular porosity that are negligible in crystalline rocks carry out conduction along vugs and cracks (Kearey et al., 2002).

Improvement in field technology and data processing has made ERT a viable tool for geological structural study on large scale investigations aside its use in environmental and geotechnical challenges (Colella *et al.*, 2004, Tamburriello *et al.*, 2008). A dipole-dipole array was employed for along 10km profile and a depth of almost 900m (Tamburriello *et al.*, 2008)

The importance of the ERT towers above most geophysical methods in geotechnics. Borehole drilling at large sites fall short of engineers' expectation because determination of rock mechanical properties are difficult to obtain from the borehole (Hassan *et al.*, 2021). Therefore the reliable approach in obtaining geotechnical parameters and reducing borehole drilling tests is the ERT. In the present dispensation, this method is seen as one of the most salient methods in geophysical survey. Its applications find relevance in archaeological,

engineering, environmental and groundwater mapping (Tsokas et al., 2009)

Measurements are taken along a line or in an area on the surface of the earth. Conversion of inferred potential differences into sounding curves or pseudo-sections of apparent resistivities, signifies resistivity variations in subsurfaces. Analyzing acquired data arising from such survey informs on the components and structures of the subsurface (Zhou, 2018). It is a 2-d non-invassive potential field method of the earth carried out at the earth surface or in boreholes to probe deepers sections if electrodes are suspended at such level (Alam *et al.*, 2024). These resistivity variations can be tied to the porosity, shape, size and connection of pores, fluid and water content of the rocks and temperature of pore water (resistivity increases with decreasing temperature) (McCarter, 1984; Lagmanson, 2005; Alam *et al.*, 2024).

Data inversion is done to reveal the image of the electrical characteristics of the subsurface.

Apparent resistivity is the resistivity of an electrically homogeneous and isotropic half-space that would produce measured Ohm's law relationship of current and potential difference for a given electrode arrangements and spacing (Wightman *et al.*, 2003; Binley, 2015). Apparent resistivity could be inferred as various resistivity's weighted average beneath electrodes. For homogeneous subsoil, apparent resistivity and true resistivity are equal (Lagmanson, 2005). Data obtained from resistivity surveys or true subsurface resistivity are basically interpreted as apparent resistivity ρ_a (Wightman, et al., 2003; Schrott and Sass, 2008). Smaller electrode distance gives more detailed reading (Schrott and Sass, 2008 and Panek *et al.*, 2008).

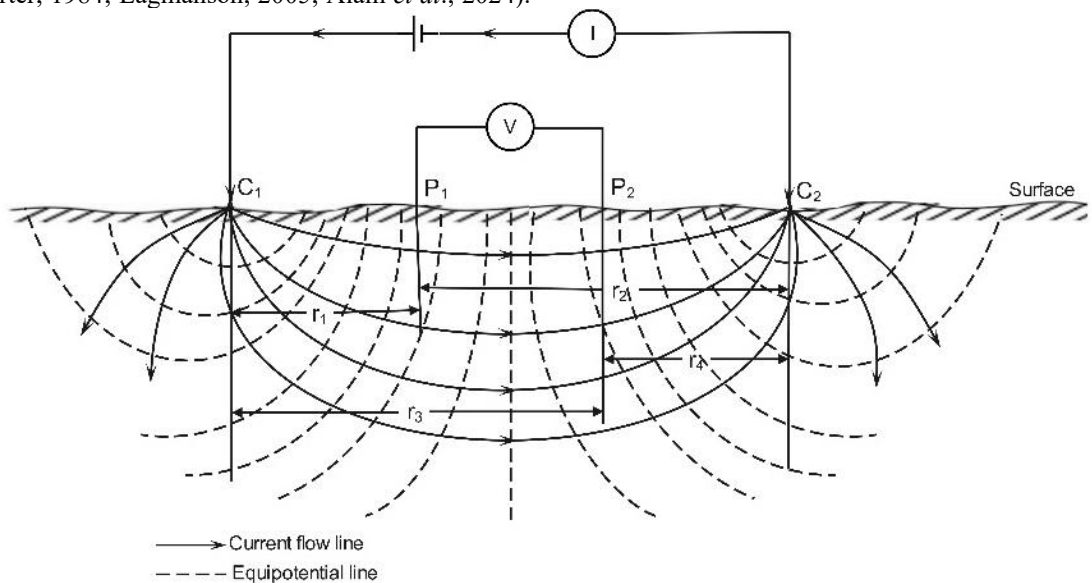


Figure 1: Wenner configuration depicting both current flow and equipotential lines

Current is injected radially from the source (electrode) for a distribution hemispherically and the resulting potential is measured by two electrodes (Zhou, 2018). Accordingly, the electric current density J of magnitude I is driven into the subsurface as represented by the expression:

$$J = \sigma E$$
Hence $\sigma E = -\sigma \nabla U$ (1)

where σ is rock conductivity, E is the electric field intensity and U is the electric potential. Electric field is the gradient of electric potential.

$$J = -\sigma \nabla U$$

$$\nabla \cdot J = 0$$

$$\nabla \cdot (\sigma \nabla U) = 0$$

$$\nabla \sigma \cdot \nabla U + \sigma \nabla^2 U = 0$$

Since this is a homogeneous medium, σ is constant, the first term varnishes, hence the equation reduces to Laplace equation

$$\nabla^2 U = 0 \tag{2}$$

Current is injected into the subsurface by current electrode $C_1(Fig.1)$ which is of different polarity from C_2 for which a given depth targeted so as to obtain the resistivity.

In view of the fact that the current electrode has a symmetric system in homogeneous isotropic medium, and a zero conductivity of the air above the electrode (Telford *et al.*, 2004)

Laplace's equation in spherical coordinate can be applied such that equation (2) becomes:

$$\frac{d^2U}{dr^2} + \frac{2}{r}\frac{dU}{dr} = 0\tag{3}$$

Multiplying through by r^2 and integrating, we have:

$$r^{2} \frac{do}{dr} = D$$

$$U = -\frac{D}{r} + F$$
(4)

where D and F are constants, since U = 0, when r approaches zero, F = 0 (Telford *et al.*, 2004)

At distance r from the electrode, the surface area of the shell is $2\pi r^2$. The current density is therefore given as:

$$J = \frac{I}{2\pi r^2} \tag{5}$$

(Zhou, 2015)

This current density is of potential gradient

$$\frac{\partial U}{\partial r} = -\rho J \tag{6}$$

(Keary et al., 2015)

The potential at the equipotential hemisphere is given as:

$$U = \frac{1\rho}{2\pi r} \tag{7}$$

(Telford et al., 2004)

The above also holds as D in equation (4) is $-\frac{l\rho}{2\pi}$

The potential at a point with current

At finite distance between two current electrodes, the potential due C_1 at P_1 is given as:

$$U_1 = \frac{I\rho}{2\pi r_1}$$

The potential due C_2 at P_1 is given as: $U_2 = -\frac{I\rho}{2\pi r_2}$

$$U_2 = -\frac{I\rho}{2\pi r_0}$$

Both are of opposite polarity.

$$U_1 + U_2 = \frac{l\rho}{2\pi} \left(\frac{1}{r_1} - \frac{1}{r_2}\right)$$
 (8)

The second potential electrode P2 will possess its potentials due C₁ and C₂ also, such that: (Telford et al, 2004):

$$\Delta U = \frac{I\rho}{2\pi} \left\{ \left(\frac{1}{r_1} - \frac{1}{r_2} \right) - \left(\frac{1}{r_3} - \frac{1}{r_4} \right) \right\}$$
 (9)
where r_1 is the distance between C_1 and P_1 , r_2 is the

distance between P₁ and P₂, r₃ is the distance between C₁ and P₂ and r₄ is the distance between P₂ and C₂ (Telford et al., 2004).

From the above, apparent resistivity ρ_a is given as:

$$\rho_a = K \frac{\Delta U}{I} = K \Delta G \tag{10}$$

where $K = 2\pi a$ is the geometric factor of the electrode array while a is the electrode spacing, ΔU is the potential difference and I is the electric current.

Wenner array is commonly used for Electrical Resistivity Tomography (ERT). It involves equal electrode spacing to get the exact reading. The Wenner array is commonly used in profiling for lateral exploration of the subsurface, like soil testing.

It is advantageous in the investigation of horizontal layering/dipping layers, shallow subsurface study and high-resolution subsurface imaging (Agada and Sonloye, 2024; Schrott and Sass, 2008).

In an attempt to determine the electrical profiling for lateral exploration, shape of the kaolin deposit, as well as volume of overburden excavation, Wenner array is used. Porosity, mineral content and temperature are the key driving factors of clay conductivity for which kaolin is an example. Clay which kaolin is a form has a resistivity value 1-100 ohm.m (Kneisel, 2003). Kaolin or China clay is a commercial clay containing majorly of the hydrated aluminosilicate clay mineral kaolinite with varying proportions of other minerals such as muscovite, quartz, feldspar (KAlSi₃O₈), and anatase. Its market value is a function of its fineness, whiteness and particle size, rheology, fluidity, colour, abrasiveness are dependent on particle size (Imery, Kaolin and Ball Clay). minerals like kaolinite (Al₂[Si₂O₅][OH]₄) are secondary geologic deposits arising from water, dissolved carbon dioxide and organic acid-driven igneous rock weathering or the chemical weathering of feldspar rich in aluminum of granite and pegmatite. It is roughly hexagonal in shape with crystal size ranging from 0.1 to 10 micrometer or more (Britannica and Imervs). Kaolin crystal formed in stacked layers is non-swelling because of the availability of hydrogen bonds that checkmate the infiltration of kaolinite crystal layers by water molecules.

Study Area

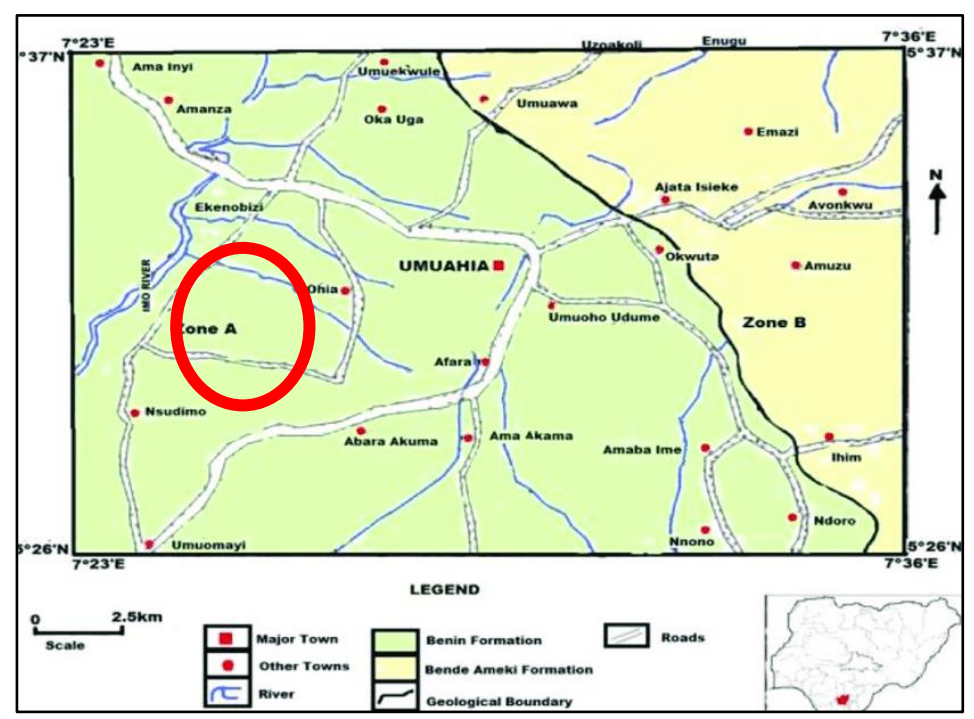


Figure 2: Map of the study area in red circle (After Onyelowe et al., 2019)

The study area in red circle in Fig. 2 is located in tha Benin Formation of the Niger Delta. The Niger Delta ages from Eocene shale Akata Formation through Agbada Formation Pliocene shale-sandstone intercalation to Recent Benin Formation which is 2km thick of significantly dominant alluvial and upper coastal sand (Avbovbo, 1978; Aigba *et al.*, 2016).

MATERIALS AND METHODS

The materials used in carrying out this research are:

i. Resistivity Meter



Plate 1: Integrated Geophysical Instrument (IGI)

This is an electronic device used to measure the flow of electric current through the ground from probes inserted at regular intervals. It gives the resistivity of the subsurface. The meter deployed in this research is the IGI (Plate 1).

- ii. Electrode: A conductor planted into the ground through which current is passed, or which is used to measure the voltage caused by the current.
- iii. Cable: A cable with a number of independent wires.
- iv. *Hammers*: For driving the electrodes into the subsurface. If the subsurface is to hard to allow for electrical conduction, some quantity of water is poured at the base of the electrodes to aid conduction.
- v. Measuring tape
- vi. Crocodile clips: These are used to hold the cables firmly on the electrodes
- vii. RES2DINVx64 Software is an inversion algorithm; packaged by Geotomo Software for 2D resistivity model determination for investigating the subsurface (Loke, 2003)

In view of the need to carry out the lateral distribution and shallow depth mapping of the area in question, Wenner array was employed for better imaging. Both the current electrodes and the potential electrodes are moved simultaneously at equidistance for measurements to be taken along a given profile.

The electrode spacing was varied from 0 to 100m in the intervals of 5m, 10m, 15m, 20m, 25m, 30m and 35m respectively.

The resistivity values were read from the IGI machine. The geometric factor was multiplied by the resistivity read from the meter and the electrode spacing. The illustration is given in equation (11) as:

 $6.2857 \times 63.6571 \times 5 \text{m} = 2000.647167$ (11)

For 5m electrode spacing, the midpoint is 7.5m. For 10m spacing the midpoint is 15m, for 15m electrode spacing, 22.5m is the midpoint. For 20m spacing, 30m is the midpoint while 38.5m remains the midpoint of 25m spacing. For 30m spacing, 45m is the midpoint while 52.5m turns out to be the midpoint of 35m when the

values are closed with four zeros. The values obtained from equation (11) above were uploaded into the RES2DINVx64 Software for electrical resistivity modeling.

RESULTS AND DISCUSSION

A total of eight (8) profiles was surveyed ranging from ERT 1 to ERT 8. The loading of the apparent resisstivity obtained into the software returned three sections of Measured Apparent Resistivity Pseudosection (MARP), Calculated Apparent Resistivity Pseudosection (CARP) and Inverse Model Resistivity Section (IMRS) with their corresponding Iterative Root Mean Square values.

The MARP informs on a two-dimensional value of resistivity needed to map variations in resistivity signifying features in the subsurface, accentuate layers, faults and other geological features. It is a pointer to further investigations.

The CARP informs on the response theory of the subsurface to the electrical resistivity survey. It helps to unify both the measured and calculated data through modeling process. It is also an essential inversion to help match measurement and the model of the subsurface while striving for precision. Pseudosections generally provide qualitative interpretation.

The IMRS helps mirror the true subsurface resistivity spread and accentuates other subsurface geological features. It is a more precise representation of the resistivity of the subsurface and shows a more detailed subsurface structures. These features of the IMRS are possible because of the root mean square (RMS) error analysis that characterizes it. Data fit is a function of the reconcilliation between the measured and calculated data - strong driving tool of IMRS which accounts for a estimation of this difference. The magnitude of the error suggests the degree of accuracy of the output (Greenhalgh *et al.*,2006). The lower the percentage error the more accurate the result is and vice-versa. This study has Root Mean Squared (RMS) error of from 10.2% to 123.8% for the eight (8) ERT profiles (Loke, 2003).

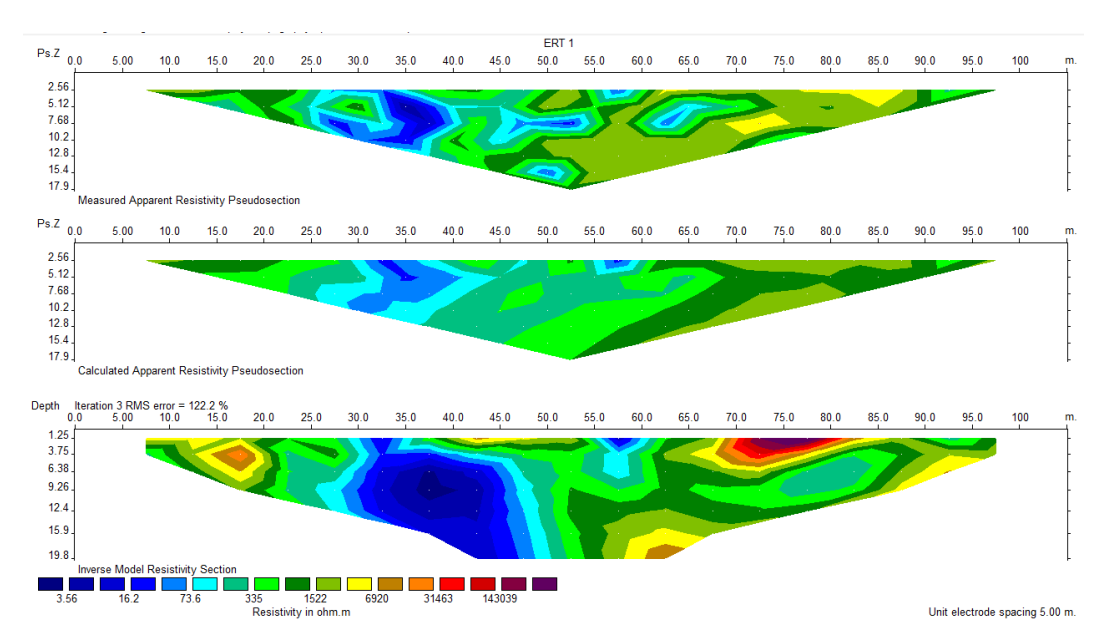


Figure 3: ERT 1 - Progressively-expansive buried prospect

Electrical resistivity tomography (ERT) comes handy in several geotechnical investigations among other uses like mineral exploration (Hassan *et al.*, 2021). The inverse model resistivity of this profile (Fig.3) shows that over a quarter of the volume of the section has kaolin deposit. A large quantity of the mineral is available between the 30m and 45m horizontal range of the profile in addition to the

depth of burial which is slightly less than 20m considering the survey outlook. A small overburden thickness of about 1.25m is required to be excavated before the presence of the deposit of interest. From the 55m to 60m horizontal range, a depth of less than 6m is of interest.

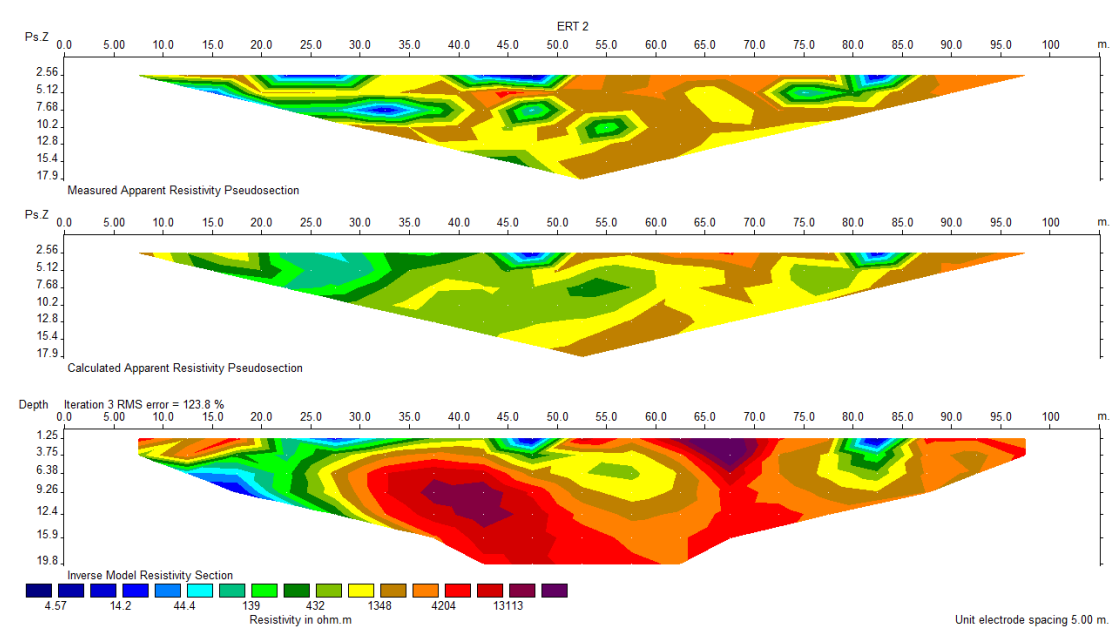


Figure 4: ERT 2 - Massive non-kaolin presence

Apart from the profile range of 25 to 30m, 45 to 50m, 60 to 70m and 80 to 85m that are located below 7m, the bulk of this profile is non kaolin deposit. Depth from 6m to

12m of 35 to 45m and 10m to 22m profile ranges are kaolin bases. Altogether, this profile does not show a promising kaolin prospect.

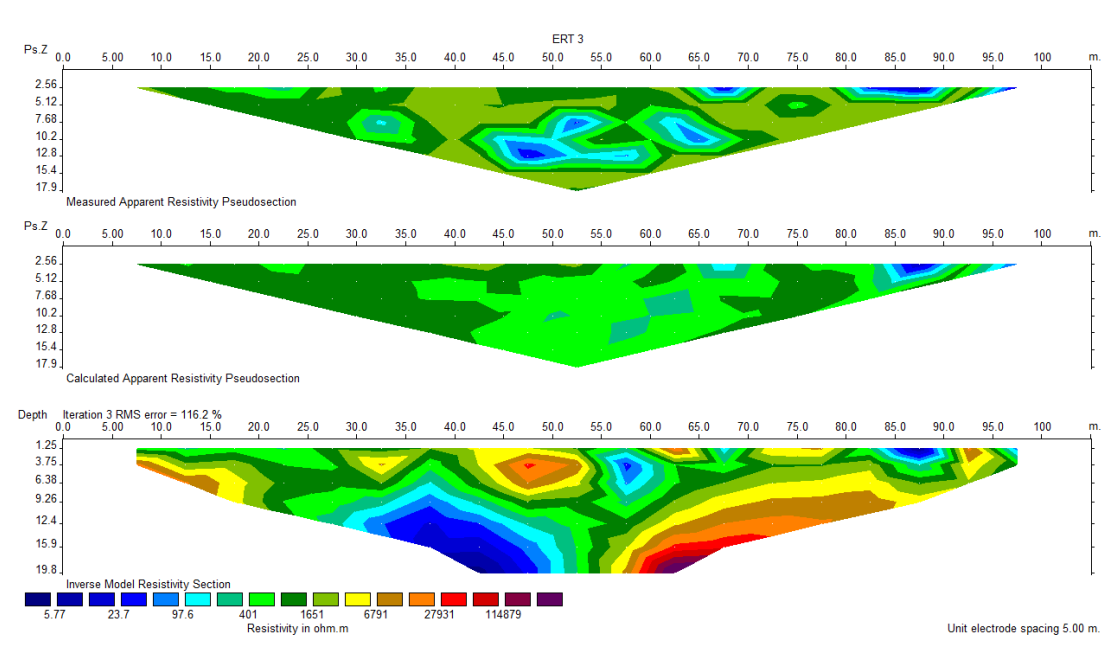


Figure 5: ERT 3 - Deeply buried kaolin south west of section

The bulk of kaolin is present at a depth below 9.2m between the range of 30 and 50m. Other minor distributions are available between 1.25 and 9m depth in

the range of 55m to 60m profile. The last patch of the mineral is available between the depth of 1.25 and 3.75m of 85 and 90m profile range.

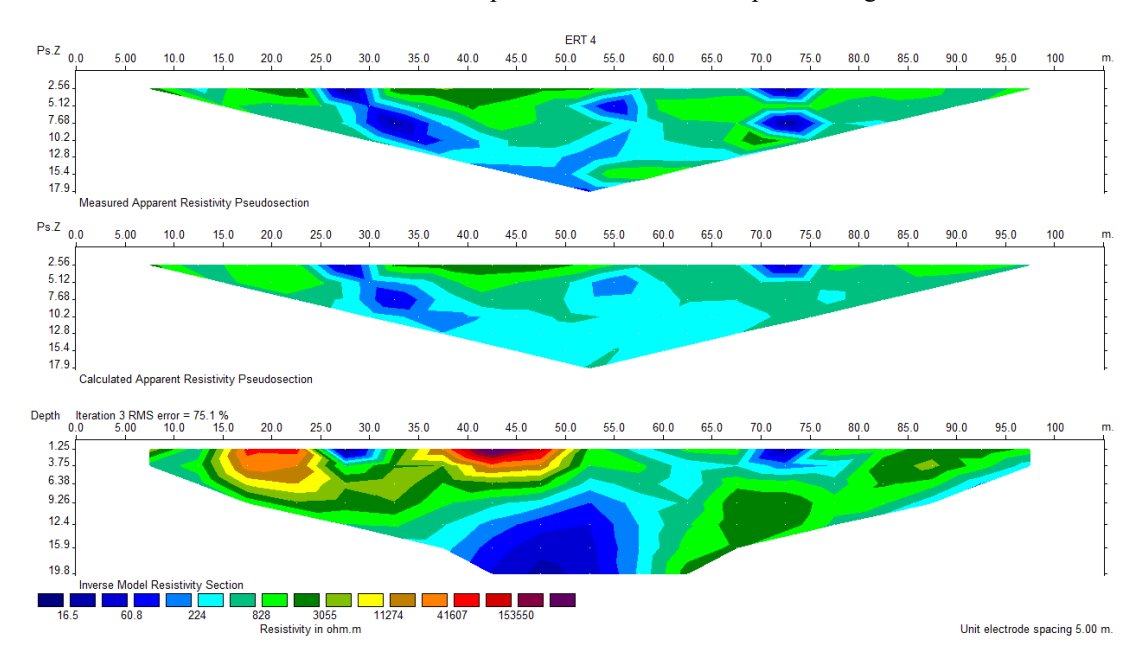


Figure 6: ERT 4 - Deeply buried kaolin south of section

The massive existence of kaolin is found below 9.26m depth and covering a range of about 35m to 57m. Other minor distributions of the mineral are found above 3.75m

with a lateral range from 25m to 30m and from 70m to 75m at a depth of 3.75m. This is a similar case scenario as seen in ERT 3.

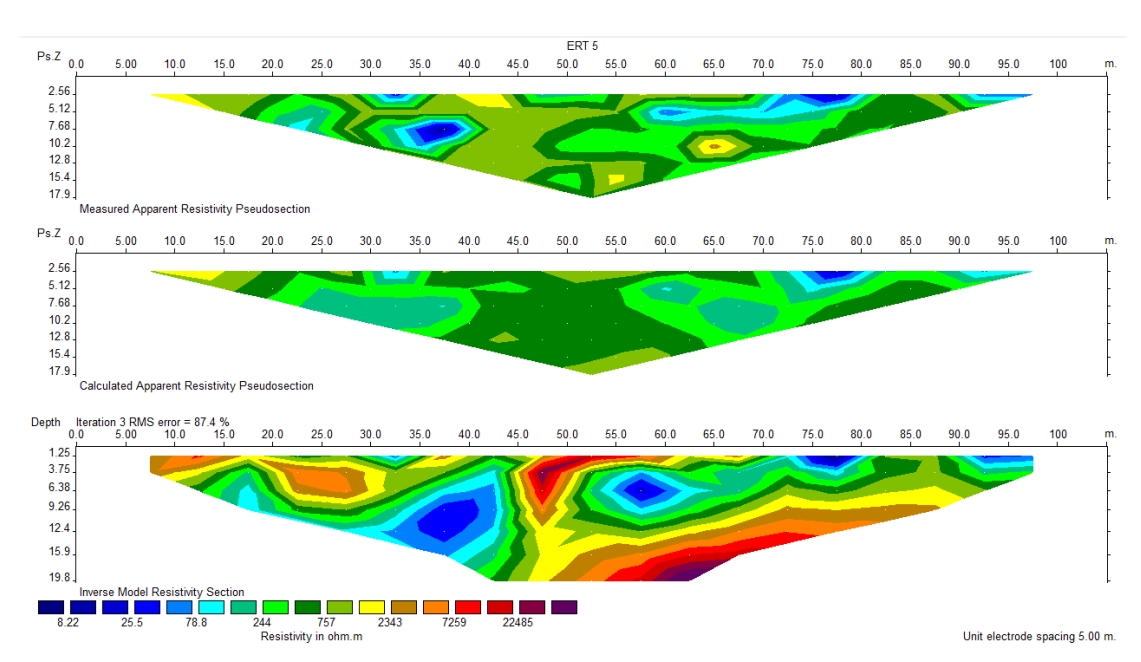


Figure 7: ERT 5 - Aligned depositions

The distribution of kaolin is in a trend suggesting reduction in depositions in patches eastward of the plot. The most concentrated deposition is found at a depth of between 3.75m and 15.9m at a profile range of 30 to

almost 45m. A deposit of kaolin also exists between 55m and 60m profile at a depth of 3.75m to 9m. Others have a profile range of 72m and 80m while the last one is between 90m and 98m both between 1.25 and 3.75m

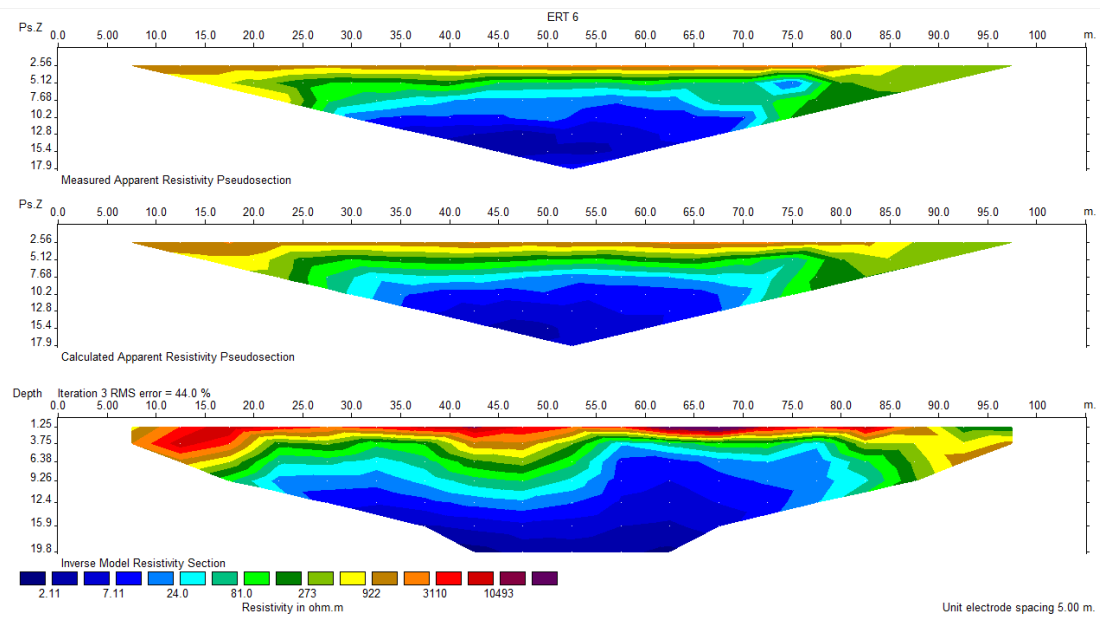


Figure 8: ERT 6 - A concentrated distribution of kaolin

The deposition of this profile is well-coordinated but deeply buried with massive overburden. Deposition spans across 20 and over 80m profile while deposition is

between a depth of 3.75m and 19.8m with the tendency of a continuation below this depth. This is a worthwhile prospect for profitable mining.

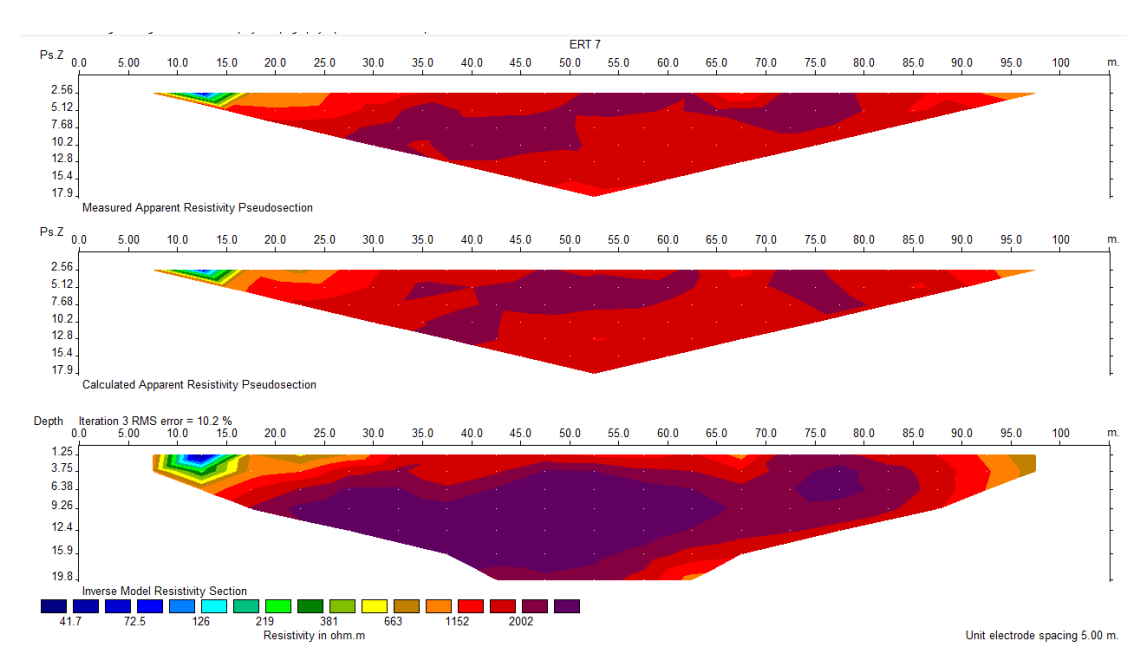


Figure 9: ERT 7 - A blend of kaolin and non-kaolin composition

The bulk of the kaolin deposit in this profile is located towards the base. This is a combination of kaolin and non-kaolin material which is almost of a homogenous blend from a depth of 3.75 to 19.8m and probably beyond

this depth. This distribution spans from 15 to 85m profile. This is accompanied by a minor deposit of a depth between 1.25 and 3.75m and a profile of 10 to 15m.

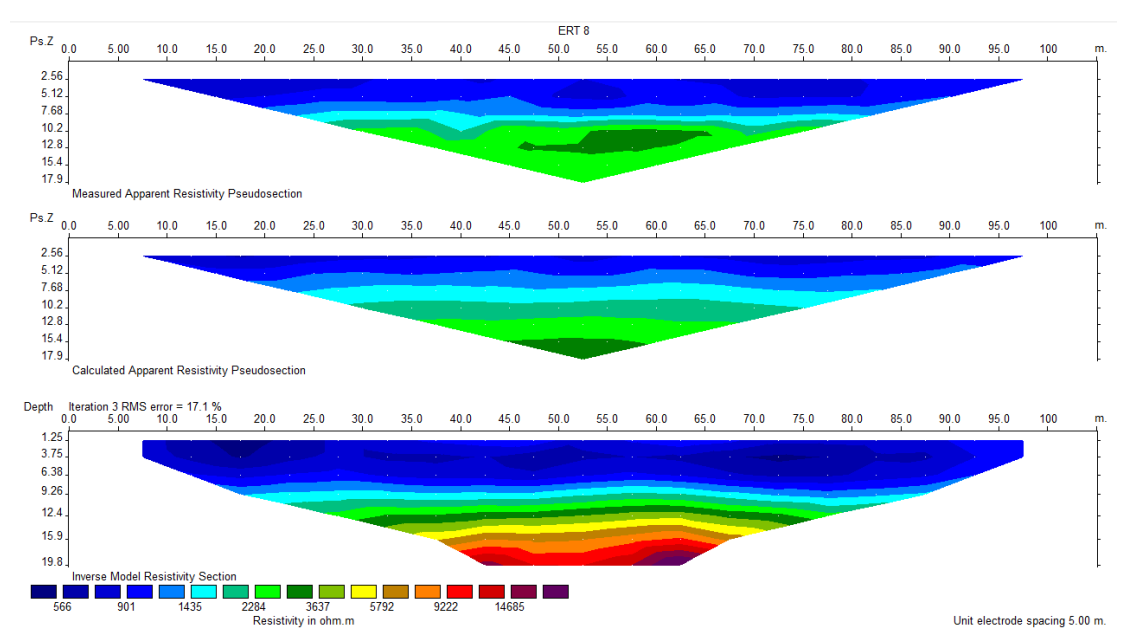


Figure 10: ERT 8 - A uniform deposition close to the surface

The profile range of between 7.5 and 97.5m shows pure kaolin deposit of a depth from 1.25 to 9.26m. The overburden is quite thin and this will allow for easy access to the prospect with little investment in time. ERT 1 (Fig. 3) has a deposit from the top to base of the profile between 30 and 50m profile range. ERT 2 (Fig. 4)

is not a promising profile and may not be attractive for excavation. ERT 3 (Fig. 5) has a deposit similar to ERT 1 but it is a deeply buried prospect that may need serious excavation before being accessed. ERT 4 (Fig. 6), ERT 3 (Fig. 5) and ERT 5 (Fig. 7) have some similarities as their depositions are dense Southeast ward.

The ERT 6 (Fig. 8) and ERT 7 (Fig. 9) are well-defined deposit at the bases of their sections and are worthwhile prospect with massive overburdens, although the latter has a blend of another rock. ERT 8 (Fig. 10) is an attractive prospect with deposit at near surface for easy exploitation with good lateral distribution.

The resistivity value of kaolin has a range of 1-100 ohm.m (Kneisel, 2003). This as observed in the various sections of the Electrical Resistivity Tomographies (ERT 1-8) that bear the colour of deep blue to light blue. This suggests the quality of kaolin available in the deposit. The clay type may range from Kaolin, sandy clay and lateritic clay although the site has some rocks of high resistivities (2002-153,650ohm.m) like sandstone of Benin Formation of the Niger Delta (Aigba *et al.*, 2016), granite and quartz.

CONCLUSION

Profiles 6 and 8 are very attractive prospects with good lateral extent distribution. Although, profile 6 is rich in kaolin, it has an overburden that requires some work input to overcome before the prospect is accessed. Profile 8 on the other hand is more attractive since it is quite close to the surface. However, construction of buildings or roads along the profile or similar ones may face some geotechnical difficulties as kaolin; an offshoot of clay has poor permeability. It is of essence to map the sub-surface of this area in a bid to guide against indiscriminate excavation. Loss of time, resources and man hour should be factored into mining this mineral before embarking on such project. Areas of characteristic lateral distribution of resource are not very common especially at near surfaces. Therefore, geophysical methods like this recommended before any excavation.

REFERENCES

Agada LE and Sonloye SA (2024). Geophysical Investigation of Building Distress in Gashua, Nigeria. *Nigerian Journal of Physics*, 33(S), 175-182. https://doi.org/10.62292/njp.v33(s).2024.271

Aigba P, Nwankwo C, and Ekine A (2016) 1-D Assessment of Formation Pressure from Transit Time and Shale Diagenesis of an Onshore Field in Niger Delta (November 17, 2016). IOSR Journal of Applied Geology and Geophysics (IOSR-JAGG), Vol. 4, Issue 6, Ver. I, 43-51

Alam MJB, Ahmed A and Alam MZ (2024) Application of Electrical Resistivity Tomography in Geotechnical and Geoenvironmental Engineering Aspect. Geotechnics 2024, 4, 399–414. https://doi.org/10.3390/geotechnics4020022

Avbovbo AA (1978) Tertiary lithostratigraphy of Niger Delta: AAPG Bulletin, Vol. 62, 295-300

Binley A (2015) Tools and techniques: DC electrical methods. In Treatise on Geophysics, 2nd ed.; Schubert, G., Ed.; Elsevier: Amsterdam, The Netherlands, 2015; Vol. 11, 233–259.

Colella A, Lapenna V, and Rizzo E (2004). High-resolution imaging of the High Agri Valley basin (Southern Italy) with Electrical Resistivity Tomography, *Tectonophysics*, 386, 29-40

Encyclopaedia Britannica Last Updated: Mar 11, 2025

Greenhalgh SA, Zhou B, Green A. (2006) Solutions, algorithms and inter-relations for local minimization search geophysical inversion. Journal of Geophysics and Engineering. 2006;3: 101-113

Hasan M, Shang Y, Meng H, Shao P and Yi X (2021) Application of electrical resistivity tomography (ERT) for rock mass quality evaluation Scientific Reports (2021) 11:23683 | https://doi.org/10.1038/s41598-021-03217-8 natureportfolio.

Imerys S.A. - 43 Quai de Grenelle, 75015 Paris Tel: +33 1 49 55 63 00

Kaolin and Ball Clay Association (UK) Par Moor Centre Par Moor Par Cornwall PL24 2SQ

Kearey P, Brooks M and Hill I (2002) An Introduction to Geophysical Exploration 3rd ed. © 2002 by Blackwell Science Ltd

Kneisel Ch (2003) Electrical resistivity tomography as a tool for geomorphological Investigations-some case studies. Zeitschrift für Geomorphologie 132, 37–49.

Lagmanson M (2005) A Presentation on Electrical Resistivity Imaging Advanced Geosciences, Inc. San Antonio, October 24, 2005

Loke MH (2003) RES2Dinv software by Geotomo Software for determining a 2D Resistivity model for subsurface investigation

McCarter WJ (1984) The electrical resistivity characteristics of compacted clays. Geotechnique 1984, 34, 263–267

Onyelowe K C, Amhadi T, Ezugwu C and Ugwuanyi H (2019) Strength of pozzolan soil blend in chemically improved lateritic soil for pavement base material purpose August 2019 International Journal of Low-

Carbon Technologies 14(3):1-7 http://dx.doi.org/10.1093/ijlct/ctz035

Pánek T, Hradecký J and Šilhán K (2008) Application of Electrical Resistivity Tomography (ERT) in the study of various types of slope deformations in anisotropic bedrock: case studies from the Flysch Carpathians Studia Geomophorlogica Carpatho Balcanica Vol. XLII, 2008: 57–73 PL ISSN 0081-6434 Landform Evolution in Mountain Areas

Schrott L and Saas O (2008) Application of field geophysics in geomorphology: Advances and limitations exemplified by case studies. Geomorphology 93, 55–73

Tamburriello G, Balasco M, Rizzo E, Harabaglia P, Lapenna V and Siniscalchi A (2008) Deep electrical resistivity tomography and geothermal analysis of Bradano foredeep deposits in Venosa area (Southern Italy): preliminary results ANNALS OF GEOPHYSICS, VOL. 51, N. 1, February 2008

Telford WM and Geldart LP, Sheriff RE (2004) Applied Geophysics *e-print* Cambridge University Press

Tsokas GN and Tsourlos PI, Papadopoulos N (2008) Electrical resistivity tomography: A flexible technique in solving problems of archaeological research *Seeing the Unseen* – Campana & Piro (eds) © 2009 Taylor & Francis Group, London, ISBN 978-0-415-44721-8 Electrical resistivity tomography Chapter September 2008 https://doi.org/10.1201/9780203889558.ch4

Wightman WE, Jalinoos F, Sirles P and Hanna K (2003) "Application of Geophysical Methods to Highway Related Problems" Federal Highway Administration, Central Federal Lands Highway Division, Lakewood, CO, Publication No. FHWA-IF-04-021, September 2003 http://www.cflhd.gov/resources/agm/

Wiwattanachang N and Giaos PH (2011) Monitoring crack development in fiber concrete beam by using electrical resistivity imaging October 2011 Journal of Applied Geophysics 75(2):294-304 http://dx.doi.org/10.1016/j.jappgeo.2011.06.009

Zhou B (2018) Electrical Resistivity Tomography: A Subsurface-Imaging Technique http://dx.doi.org/10.5772/intechopen.81511